CellPress OPEN ACCESS

Trends in Biotechnology

Research Article

Production of phosphorylated and functional α_{S1}-casein in *Escherichia coli*

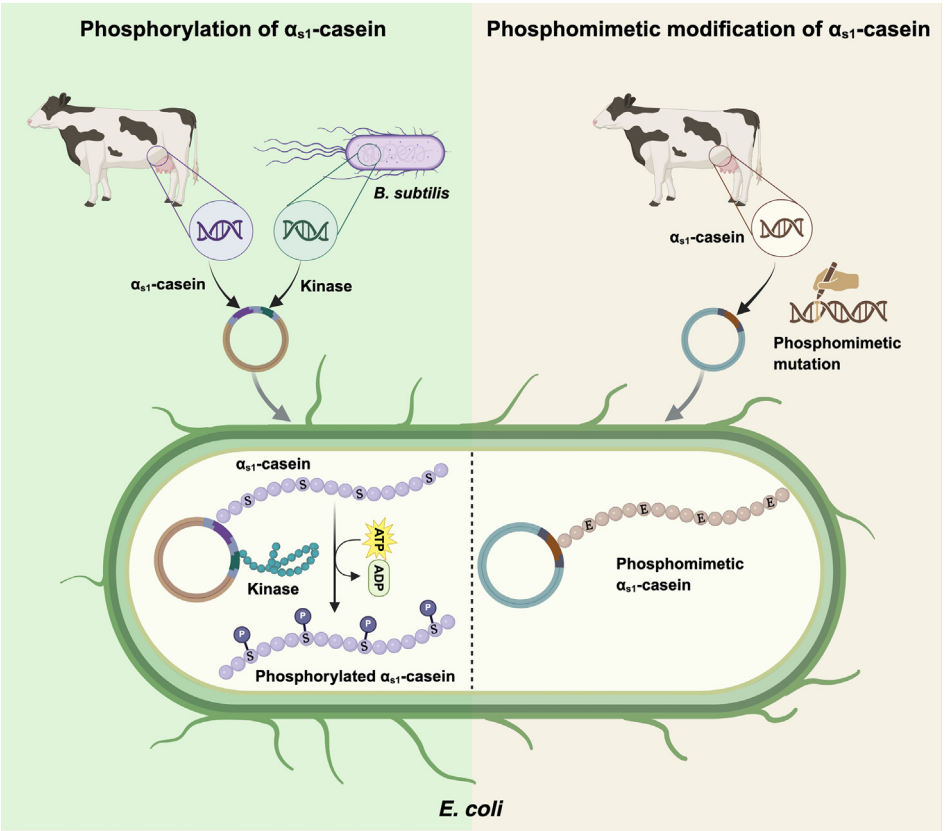

The study demonstrates two strategies, phosphorylation of α_{s1}-casein using *Bacillus subtilis* kinases and phosphomimetic substitution of α_{s1}-casein, to generate functional recombinant α_{s1}-casein in *Escherichia coli*. Mass spectrometry and two-dimensional gel electrophoresis (2DE) confirm site-specific phosphorylation, while functional assays reveal calcium-binding capacity and structural mimicry, offering a foundation for animal-free dairy protein innovation.

Suvasini Balasubramanian, Golnaz Mobasseri, Lei Shi, Carsten Jers, KohlerJulie Bonne Køhler, Adeline Boire, Claire Berton-Carabin, Ivan Mijakovic, Peter Ruhdal Jensen

Ivan.Mijakovic@chalmers.se
(I. Mijakovic)
perj@food.dtu.dk
(P.R. Jensen).

Highlights

A major challenge in producing caseins in microbial systems is their reliance on essential post-translational modifications, particularly phosphorylation. Phosphorylation of serine residues is critical for calcium binding and the formation of colloidal calcium phosphate nanoclusters, both of which are fundamental to casein micelle assembly and contribute to their functional and nutritional properties in dairy systems.

A phosphorylation pattern similar to bovine α_{s1}-casein was achieved in recombinant α_{s1}-casein through the use of *Bacillus subtilis* kinases PrkD and YabT.

Phosphomimetic casein offers a feasible alternative to phosphorylation while maintaining functional properties.

Both phosphorylated and phosphomimetic caseins exhibited significantly higher calcium-binding capacity compared with unphosphorylated caseins.

Trends in Biotechnology, Month 2025, Vol. xx, No. xx
https://doi.org/10.1016/j.tibtech.2025.05.015

© 2025 The Author(s). Published by Elsevier Ltd. This is an open access article under the CC BY license (http://creativecommons.org/licenses/by/4.0/).

Trends in Biotechnology

CellPress OPEN ACCESS

Research Article

Production of phosphorylated and functional α_{S1}-casein in *Escherichia coli*

Suvasini Balasubramanian[1,2,6], Golnaz Mobasseri[3,6], Lei Shi[3], Carsten Jers[2], Julie Bonne Køhler[2], Adeline Boire[4], Claire Berton-Carabin[4,5], Ivan Mijakovic[2,3,*], and Peter Ruhdal Jensen[1,*]

While the demand for milk proteins is on the rise, sustainability concerns dictate a reduction in animal-based agriculture. Microbial cell factories can be a viable alternative, but their inability to phosphorylate recombinant caseins is a major bottleneck, since phosphorylation is needed for calcium binding and functionality. We propose a solution that involves engineering bacteria to co-express bacterial protein kinases, resulting in recombinant caseins with the native phosphorylation pattern and functional properties. We successfully phosphorylated α_{s1}-casein in *Escherichia coli* using bacterial kinases, achieving phosphorylation at all native sites. To complement this approach, we developed an alternative phosphomimetic strategy by substituting serine residues with aspartate to mimic phosphorylation. Structural and functional characterization of all the phosphorylated/phosphomimetic recombinant α_{s1}-caseins demonstrated properties comparable with those of bovine α-casein, including calcium-binding affinity, digestibility, and structural integrity. Notably, phosphomimetic α_{s1}-casein may offer a simpler system, while phosphorylated casein more closely resembles bovine casein. This approach has significant implications for the development of alternative protein sources, addressing both sustainability and functional demands in the food industry.

Technology readiness

Achieving the correct phosphorylation pattern is a significant challenge in utilizing recombinant caseins for food applications, as it is critical for their functionality and poses a major barrier to commercialization. The use of bacterial kinase co-expression to phosphorylate α_{s1}-casein, mimicking the native phosphorylation pattern, and an alternative phosphomimetic strategy to bypass the requirement for phosphorylation have been successfully established for the first time. These caseins were tested for their ability to bind calcium at the laboratory scale. Calcium-binding capability is essential for the formation of casein micelles, which are critical for casein functionality in food matrices. As this has been demonstrated at the laboratory scale, the current Technology Readiness Level (TRL) is assessed at 4.

Introduction

Milk proteins are an integral part of human nutrition and exhibit an array of functional properties that significantly contribute to the taste, texture, and flavor of various dairy products [1–3]. These proteins, primarily fractionated into caseins and whey proteins, are highly valued for their nutritional profile and bioavailability, making them a preferred source of protein for both infants and adults [4]. However, despite their nutritional benefits, conventional dairy production is often criticized for its environmental impact and ethical concerns regarding animal welfare [5,6]. As the demand for dairy proteins continues to rise, these challenges underscore the need for alternative and sustainable milk production methods.

The global casein market was valued at US$2.7 billion in 2023, with projections indicating growth at a compound annual growth rate of 6.3%, reaching US$4.9 billion by 2033 [7]. Caseins are particularly valued in the food and pharmaceutical industries due to their biocompatibility and versatility. In food applications, they contribute to foaming, emulsification, and stabilization, while, in pharmaceuticals, their solubility, gelation, and binding properties make them ideal for drug formulation [8,9]. In addition, caseins are a preferred nutraceutical for sports professionals and individuals with specific nutritional needs. However meeting the growing demand for casein-based products requires an increase in dairy production, which, in turn, exacerbates environmental concerns and reinforces the need for alternative production technologies.

[1]Microbial Biotechnology and Biorefining, National Food Institute, Technical University of Denmark, Kongens Lyngby, Denmark
[2]Novo Nordisk Foundation Center for Biosustainability, Technical University of Denmark, Kongens Lyngby, Denmark
[3]Systems and Synthetic Biology Division, Department of Life Sciences, Chalmers University of Technology, Gothenburg, Sweden
[4]INRAE, UR BIA, 144000, Nantes, France
[5]Laboratory of Food Process Engineering, Wageningen University and Research, 6700 AA Wageningen, The Netherlands
[6]Co-first authors

*Correspondence:
Ivan.Mijakovic@chalmers.se (I. Mijakovic) and perj@food.dtu.dk (P.R. Jensen).

© 2025 The Author(s). Published by Elsevier Ltd. This is an open access article under the CC BY license (http://creativecommons.org/licenses/by/4.0/).

In this context, precision fermentation and cellular agriculture offer promising alternatives for producing sustainable animal proteins [10–12]. Microorganisms have long been utilized as cell factories in food and pharmaceutical applications, facilitating the production of dietary supplements, enzymes, and other biomolecules [13–16]. Advances in biotechnology have expanded the repertoire of microbial hosts beyond traditional model organisms, allowing the reengineering of diverse microbial species for recombinant protein production [17]. This has led to the successful commercial-scale expression of whey proteins through precision fermentation, with these proteins now marketed at a premium [18–20].

However, achieving functional casein production via microbial systems remains a significant challenge. One of the primary obstacles in recombinant casein production is the need for proper post-translational modifications (PTMs), particularly phosphorylation. While whey proteins, particularly β-lactoglobulin, can be expressed efficiently in microbial hosts due to their lack of PTMs, such as phosphorylation or glycosylation, caseins require precise phosphorylation to retain their functional properties, especially their ability to bind amorphous calcium phosphates and form micelles. Prokaryotic hosts, such as *E. coli,* lack the specificity and regulation required for accurate mammalian protein phosphorylation, whereas eukaryotic hosts, such as yeasts and fungi, introduce non-native modifications, including mannosylation and glycosylation, which do not occur in bovine α- and β-caseins [21–24]. In addition, these hosts contain intracellular and extracellular proteases that can degrade recombinant proteins [12]. Due to their flexible and unstructured nature, caseins are particularly susceptible to proteolytic degradation [25]. Along with incomplete phosphorylation, these challenges hinder the successful production of bovine identical caseins.

Caseins are a unique family of phosphoproteins that constitute the major protein fraction of milk, having a crucial role in mineral sequestration, structural assembly, and molecular interactions within dairy systems [26,27]. Unlike many globular proteins, caseins are intrinsically disordered, lacking a defined tertiary structure and exhibiting high net charge and low hydrophobicity, which allows them to interact dynamically with multiple proteins [28]. This structural plasticity is largely attributed to their high proline content (9% in α_{s1}-casein and 18% in β-casein), along with the absence of disulfide bridges, resulting in an open, flexible conformation [29]. The intrinsically disordered nature of caseins is crucial to their function, providing key advantages, such as mineral binding and chaperone-like properties [30,31].

This key functional aspect of caseins, their ability to bind calcium, is primarily mediated by phosphoseryl (SerP) residues. The strength of this interaction depends on the number and arrangement of these residues, particularly in calcium-sensitive caseins, such as α_{s2}-casein (10–13 SerP per molecule), α_{s1}-casein (eight to nine SerP), and β-casein (five SerP) [30,32–34]. When three or more SerP residues are clustered, they form phosphate centers (PCs) that enhance calcium-binding capacity and facilitate micelle formation [35–37]. To effectively sequester calcium phosphate, PCs must be present in excess compared with calcium phosphate, ensuring micelle stability and thermodynamic balance in milk [38]. The casein micelle, ~100 nm in radius, is an assembly of nanoclusters, each containing ~50 PCs [39], which collectively promote calcium phosphate transport and aid neonatal digestion.

In dairy applications, micellar structures are particularly important for cheese production, where proteolysis of κ-casein under optimal conditions destabilizes the micelles, leading to aggregation and curd formation [40,41]. Studies with partially and fully dephosphorylated caseins have demonstrated their inability to form micelles, because dephosphorylated caseins exhibit reduced calcium-binding capacity [42]. Furthermore, when incorporated with native caseins, dephosphorylated

caseins disrupt the gel network, affecting the overall texture of dairy products [43]. These findings underscore the necessity of phosphorylation for casein functionality, particularly in dairy processing and cheese manufacturing.

Previous attempts to phosphorylate recombinant β-casein analogs using casein kinase II in *E. coli* achieved high phosphorylation levels and biomimetic micelle formation, although efficiency was lower for native casein sequences [44,45]. In addition, biomimetic micelles differed structurally from native micelles, particularly in their kinetics of calcium sequestration and aggregation behavior [44]. A breakthrough in microbial production of functional milk proteins, specifically in achieving high levels of native phosphorylation patterns in biologically identical caseins, would revolutionize the dairy industry, reducing the need for intensive animal farming while improving sustainability and animal welfare.

In this study, we engineered *E. coli* to phosphorylate α_{s1}-casein, both *in vitro* and *in vivo*, using bacterial kinases. Various serine/threonine protein kinases were assessed for their specificity toward bovine α_{s1}-casein. Phosphorylation sites were validated on *in vitro* phosphorylated samples using liquid chromatography-mass spectrometry (LC-MS), and subsequently assessed on *in vivo* phosphorylated variants by two-dimensional gel electrophoresis (2DE). Ca^{2+} binding and fluorescence spectroscopy analyses were conducted to assess the structural and functional similarity of recombinant caseins to bovine caseins. These results provide insights that could contribute to optimizing recombinant casein production and enable future advances in precision fermentation for sustainable dairy alternatives.

Results

Expression of proteins

To identify suitable kinases for phosphorylating milk proteins, we targeted enzymes with specificity for the S-*x*-E/pS motif (where E/pS represents glutamic acid or phosphorylated serine, and *x* is any amino acid). GEF-CK, which phosphorylates milk proteins in bovine mammary glands, served as a reference. Based on this, human and bovine Fam20C kinases were selected [46,47]. However, producing complex mammalian proteins, such as Fam20C, in bacterial systems is challenging and, to date, successful expression of human Fam20C has only been achieved in human cell lines [48]. As expected, attempts to express two different versions of Fam20C kinase in *E. coli* were unsuccessful due to protein aggregation (Figure S1 in the supplemental information online). Consequently, we turned to well-characterized bacterial Ser/Thr kinases that are more suitable for expression in *E. coli*. We chose three Hanks-type kinases [49,50] from *Bacillus subtilis*: PrkC, PrkD, and YabT [51]*, which* are known for their relaxed specificity toward phosphorylated residues. For PrkC and PrkD, the active domains can be expressed without regulatory domains (Figure 1A), ensuring constitutive kinase activity. Expression of α_{s1}-casein, and the kinases were controlled under IPTG inducible T7/T5 promoter at optimal conditions. To assist with folding and solubility, kinases were co-expressed with chaperones GroES/EL. SDS-PAGE analysis revealed distinct bands of the proteins (Figure 1B,C). Despite the theoretical molecular weight of 27.4 kDa with a 6xHis-tag, α_{s1}-casein was detected at a higher mass of ~35 kDa, consistent with previous studies [52,53].

In vitro and *in vivo* phosphorylation of recombinant α_{s1}-caseins

Given that α_{s1}-casein ($R\alpha_{s1}$) expressed in *E. coli* did not have any phosphorylation, we assessed whether these kinases could phosphorylate the purified $R\alpha_{s1}$ using an *in vitro* assay based on incorporation of radioactive ^{32}P. All three bacterial kinases were capable of phosphorylating $R\alpha_{s1}$ *in vitro* to some extent, with PrkD and YabT yielding the strongest signals, along with evidence of their enzymatic activity through autophosphorylation (Figure 1C). Next, we verified the identity

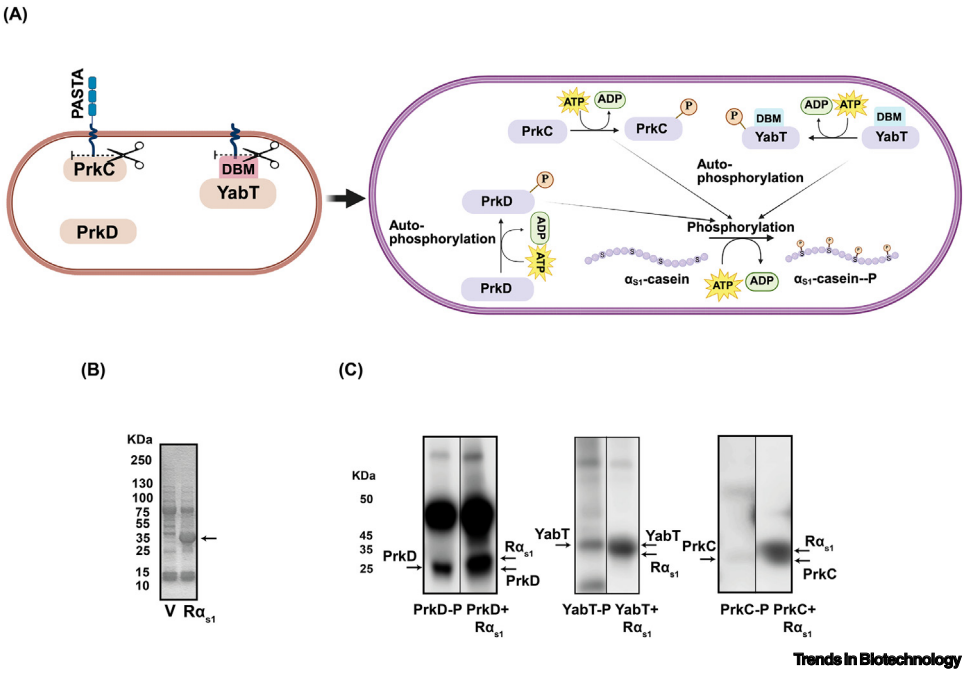

Figure 1. *In vitro* phosphorylation of α_{s1}-casein by bacterial kinases PrkD, YabT, and PrkC. (A) Schematic of engineered active kinase domains from *Bacillus subtilis* native form into *Escherichia coli* co-expressing form, achieved by clipping transmembrane helices and PASTA domains. For YabT, both the domain and the DNA-binding motif (DBM) were retained. (B) SDS-PAGE of total protein extracts of strain expressing α_{s1}-casein ($R\alpha_{s1}$). (C) Autoradiograph revealing the phosphorylation signals from *in vitro* kinase assays. The first lane of each gel shows the respective kinases (PrkD, YabT, and PrkC) without $R\alpha_{s1}$, highlighting the autophosphorylation bands of each kinase. The second lane of each gel displays the phosphorylation of $R\alpha_{s1}$ by the specific kinases. Arrows point to the respective protein bands. (A) created using BioRender (biorender.com).

of amino acid residues on α_{s1}-casein phosphorylated by each kinase using LC-MS. PrkD phosphorylated all nine native sites [46,54,55], and YabT phosphorylated eight of them (Figure 2A), demonstrating that these two kinases not only exhibited the highest phosphorylation activity, but also closely replicated the native phosphorylation pattern. PrkC phosphorylated only one native residue and, thus, was not investigated further. All bacterial kinases also phosphorylated several nontarget residues in α_{s1}-casein (Figure 2A). Following *in vitro* phosphorylation and phosphoprotein analysis, the kinases that achieved successful phosphorylation at the native serine sites (PrkD and YabT) were chosen for *in vivo* phosphorylation. Achieving phosphorylation during protein expression removes the need for separate *in vitro* phosphorylation steps, reducing time, cost, and complexity in downstream processing.

PrkD and YabT were co-expressed with α_{s1}-casein (PrkD, $R\alpha_{s1}$-PD; YabT, $R\alpha_{s1}$-YT) in a pET15b vector under the T7 promoter with the induction of IPTG at optimal conditions (Figure 2B). All three α_{s1}-caseins($R\alpha_{s1}$, $R\alpha_{s1}$-PD, and $R\alpha_{s1}$-YT) were purified using affinity chromatography, and separated on a 2D gel to visualize the phosphorylation pattern and total protein. Considering the isoelectric range relevant for casein, an 11-cm immobilized pH gradient (IPG) strip (pH 4–7) was used for isoelectric focusing, followed by separation by SDS-PAGE in a second-dimension gel. Pro-Q diamond staining followed by SYPRO Ruby total protein staining enabled mapping of the kinase phosphorylation. Pro-Q diamond staining of the 2D gels in Figure 2C revealed that, when co-expressed with either PrkD or YabT, α_{s1}-casein was heavily phosphorylated, yielding a signal comparable with that of commercial native phosphorylated α-casein (α-Cn). The total

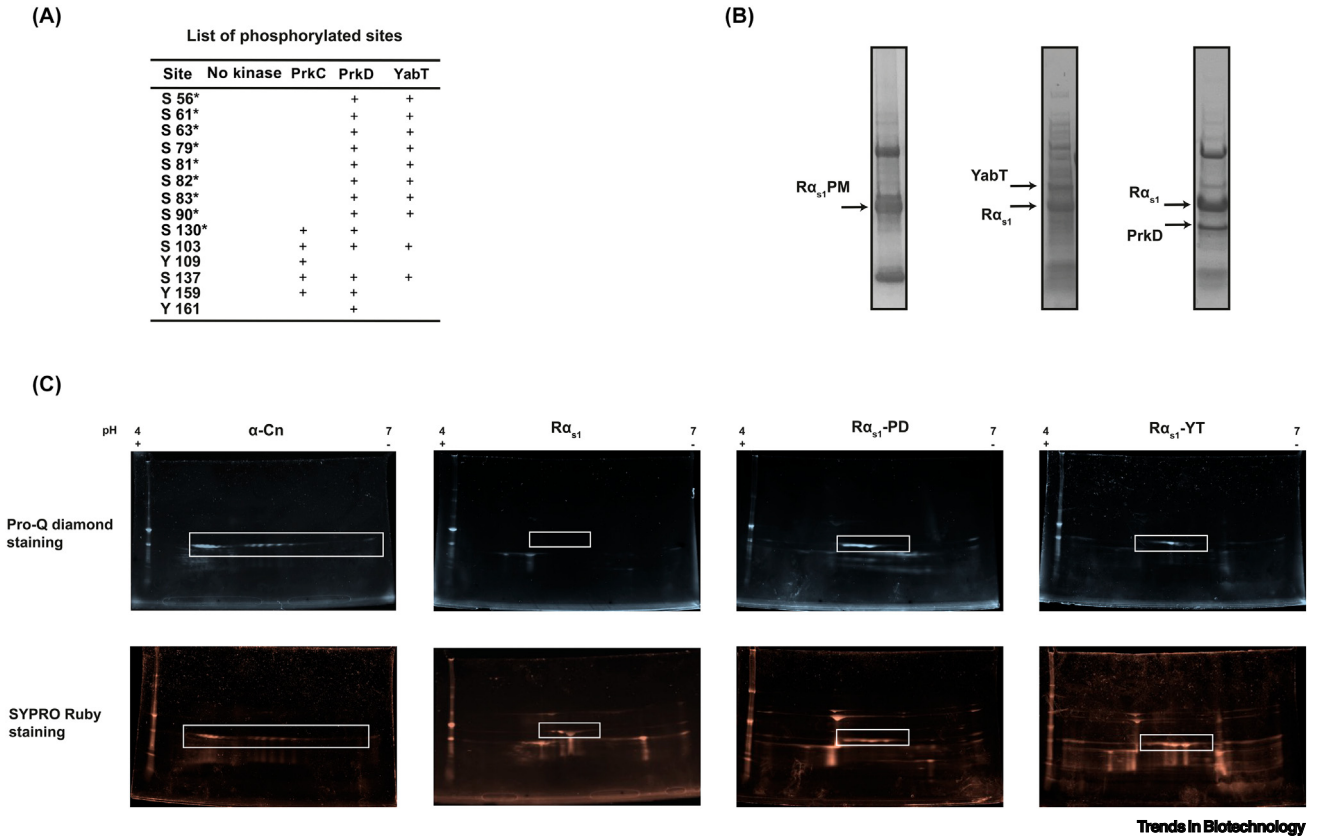

Figure 2. Phosphorylation of α_{s1}-casein. (A) Native and non-native sites from *in vitro* phosphorylation of α_{s1}-casein, identified using liquid chromatography-mass spectrometry (LC-MS). (B) SDS-PAGE of total protein extracts of lysate from *Escherichia coli* expressing phosphomimetic α_{s1}-casein (Rα_{s1}-PM) and *E. coli* co-expressing α_{s1}-casein and respective kinases [YabT (Rα_{s1}-YT) and PrkD (Rα_{s1}-PD)]. Arrows point to the respective protein bands. (C) pH 4–7 immobilized pH gradient (IPG) strips were used for isoelectric focusing, followed by SDS-PAGE in the second dimension and staining with phosphoprotein stain Pro-Q diamond and total protein stain SYPRO Ruby for mapping phosphorylation levels induced by the different kinases relative to the total protein. α-casein (α-cn) was used as a positive control.

protein stain with SYPRO Ruby revealed five and four isoforms of Rα_{s1}-PD, and Rα_{s1}-YT, respectively. Of these, four in Rα_{s1}-PD, and two in Rα_{s1}-YT were phosphorylated based on the signal from Pro-Q diamond staining, while the unphosphorylated Rα_{s1}-casein led to no signal.

One strategy to compensate for phosphorylation loss is the use of phosphomimetic mutations, where negatively charged glutamic acid or aspartic acid residues replace serine phosphorylation sites. Phosphomimetic mutants on other proteins have shown structural and functional similarities to phosphorylated serines by mimicking conformational states and enhancing mineral binding [56,57].

In this study, phosphomimetic α_{s1}-casein (Rα_{s1}-PM) was generated by substituting the eight potential serine residues with aspartic acid and expressed in the bacterium (Figure 2B). Along with Rα_{s1}-PM, the phosphorylated caseins (Rα_{s1}-PD and Rα_{s1}-YT) were also examined to determine whether these recombinant α_{s1}-caseins retained functional properties relevant to food applications.

Functional characterization of recombinant α_{s1}-caseins

Digestibility analysis of recombinant α_{s1}-caseins. The digestibility of all the recombinant α_{s1}-caseins, including *in vitro* phosphorylated samples, was assessed using simulated gastrointestinal fluids [simulated gastric fluid (SGF) and simulated intestinal fluid (SIF)]. The INFOGEST static *in vitro*

digestion protocol was adapted to visualize the kinetics of the protein hydrolysis [58]. Figure 3 shows protein degradation during the oral, gastric, and intestinal phases with time-resolved sampling on an SDS-PAGE gel. By the end of the intestinal phase, all proteins were completely digested. The digestion profiles of all the recombinant α_{s1}-caseins were qualitatively similar, except for the phosphomimetic variant, which exhibited slightly higher stability in SGF. Overall, this aligns with previous studies on bovine α-casein, which show rapid hydrolysis during digestion [59].

Calcium binding affinity of recombinant α_{s1}-casein. To assess the impact of phosphorylation on mineral binding, we measured the calcium-binding affinity of Rα_{s1}-PD, Rα_{s1}-YT, and Rα_{s1}-PM using a colorimetric assay (Figure 4). Binding affinity was determined by quantifying the chromogenic complex formed between free calcium ions and O-cresolphthalein at 575 nm. The difference in the bound calcium ions between the phosphorylated and dephosphorylated bovine

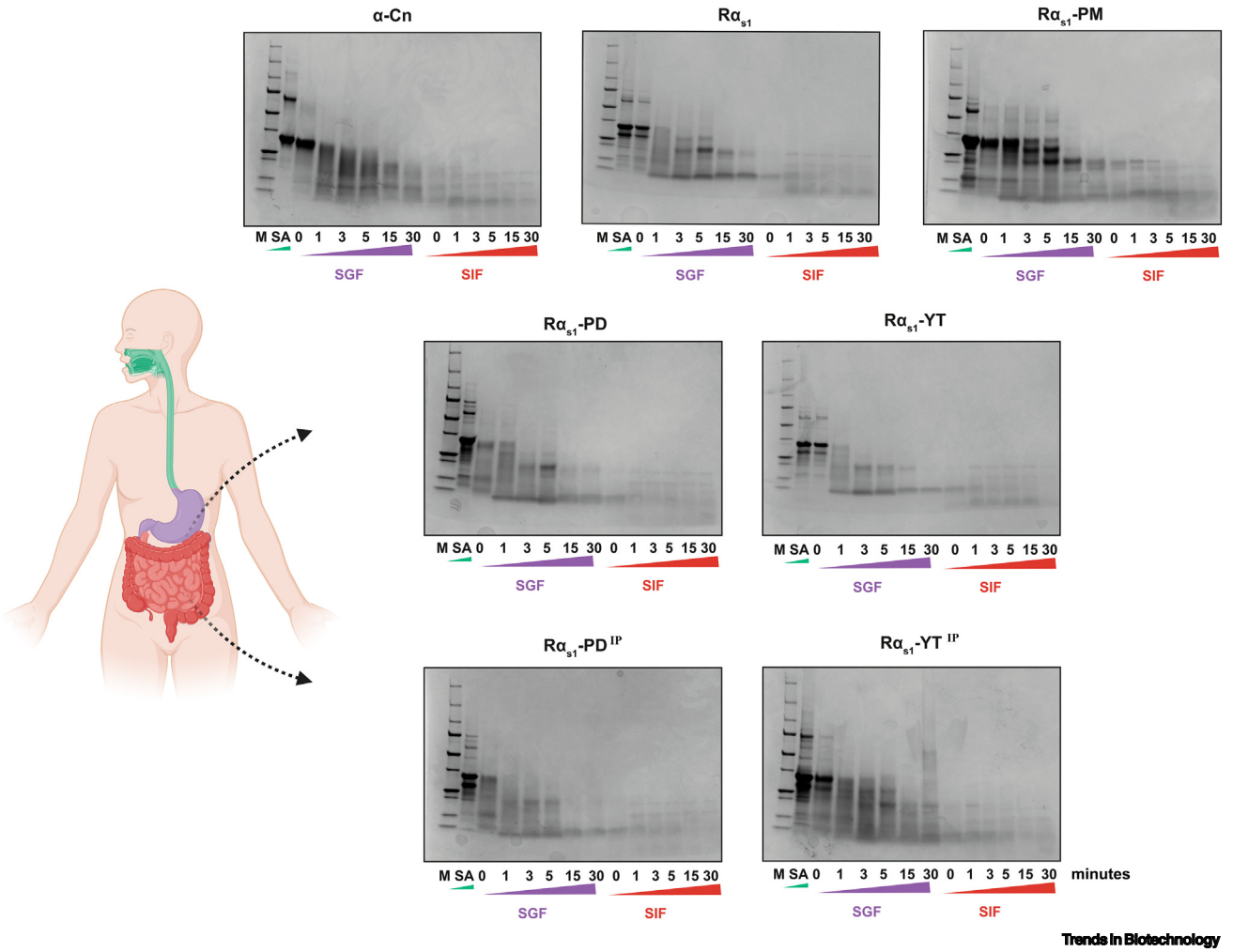

Figure 3. *In vitro* simulated gastrointestinal digestion of caseins. The oral phase (green), gastric phase (purple), and intestinal phase (red) are indicated. Digested samples were analyzed by SDS-PAGE. α-casein (α-cn) was used as a positive control. *In vitro* phosphorylated casein samples are indicated as IP. Schematic of human gastrointestinal tract created using BioRender (biorender.com). Abbreviations: SA, simulated salivary fluid; SGF, simulated gastric fluid; SIF, simulated intestinal fluid.

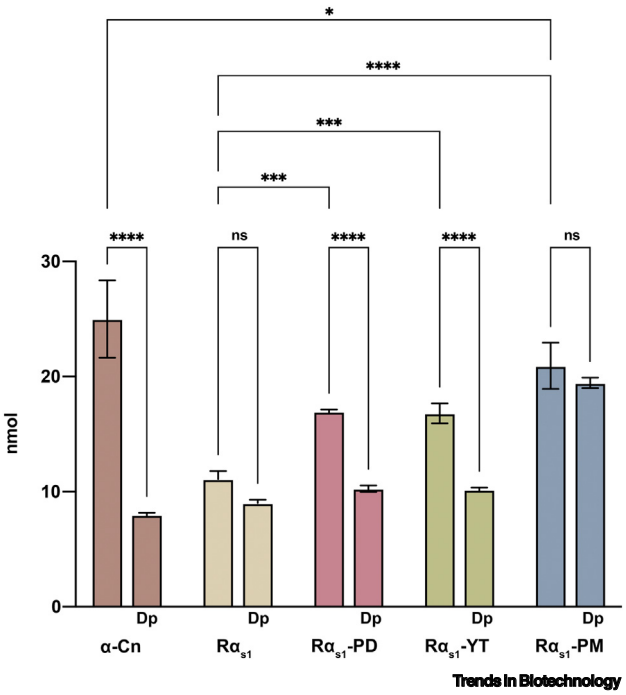

Figure 4. Calcium-binding assay. The bar graph depicts the calcium binding affinity of the protein samples. α-cn (α_{s1}- and α_{s2}-casein) was used as a positive control. Y-axis represents calcium-binding affinity as a function of nmol per mg of protein. *In vivo* phosphorylated α_{s1} caseins were used in the study. Data are mean ± standard deviation (SD) (n =3); analyzed using two-way ANOVA followed by Šídák's multiple comparisons test: *P <0.05, ***P <0.001, ****P <0.0001, ns, not significant. Comparisons were made between control α-cn and recombinant α_{s1} caseins, and recombinant α_{s1} caseins with their dephosphorylated counterparts. Abbreviation: Dp, dephosphorylated.

α-casein demonstrated the role of phosphorylation in mineral binding. While nonphosphorylated serine residues can bind calcium to some extent, phosphorylation substantially enhances this capacity [60,61].

Results indicated that phosphorylation significantly enhanced calcium binding, as shown by the increased Ca^{2+} affinity in phosphorylated casein compared with the unphosphorylated α_{s1}-casein. Dephosphorylated caseins exhibited a notable reduction in binding affinity, demonstrating the critical role of phosphorylation in mineral interactions. Interestingly, the phosphomimetic variant (Rα_{s1}-PM) exhibited stronger calcium binding. This can be attributed to the negative charge of the phosphomimetic residues facilitating a stronger electrostatic interaction between the protein and the Ca^{2+} ions, which are naturally present in phosphorylated proteins. This observation aligns with previous findings, where aspartate has been shown to enhance calcium binding in α-lactalbumin [62,63]. Substituting potential serine residues with aspartates could partly mimic phosphorylated serine.

Structural characterization using intrinsic fluorescence. To further investigate the structural effects of *in vivo* phosphorylation and phosphomimetic modifications, we analyzed the intrinsic fluorescence emission spectra of the recombinant α_{s1}-caseins. Fluorescence emission primarily arises from aromatic residues phenylalanine (Phe), tryptophan (Trp), and tyrosine (Tyr), with Trp typically dominating the emission spectra due to its longer emission wavelengths, higher extinction coefficient, and greater quantum yield compared with Phe and Tyr [64]. Prior research on α_{s1}-casein showed that Trp179 (164 without the signal peptide) accounts for ~80% of its conformational changes, with calcium concentration having a critical role in modulating fluorescence intensity [65]. Given that Trp is highly sensitive to its surrounding environment, distinct fluorescence patterns were observed across the proteins (Figure 5A–C). The 3D excitation (Ex)-emission (Em) matrix (EEM) for α_s-caseins highlighted Trp (Ex. 290 nm, Em. 340–350 nm) and Tyr (Ex. 275 nm, Em.

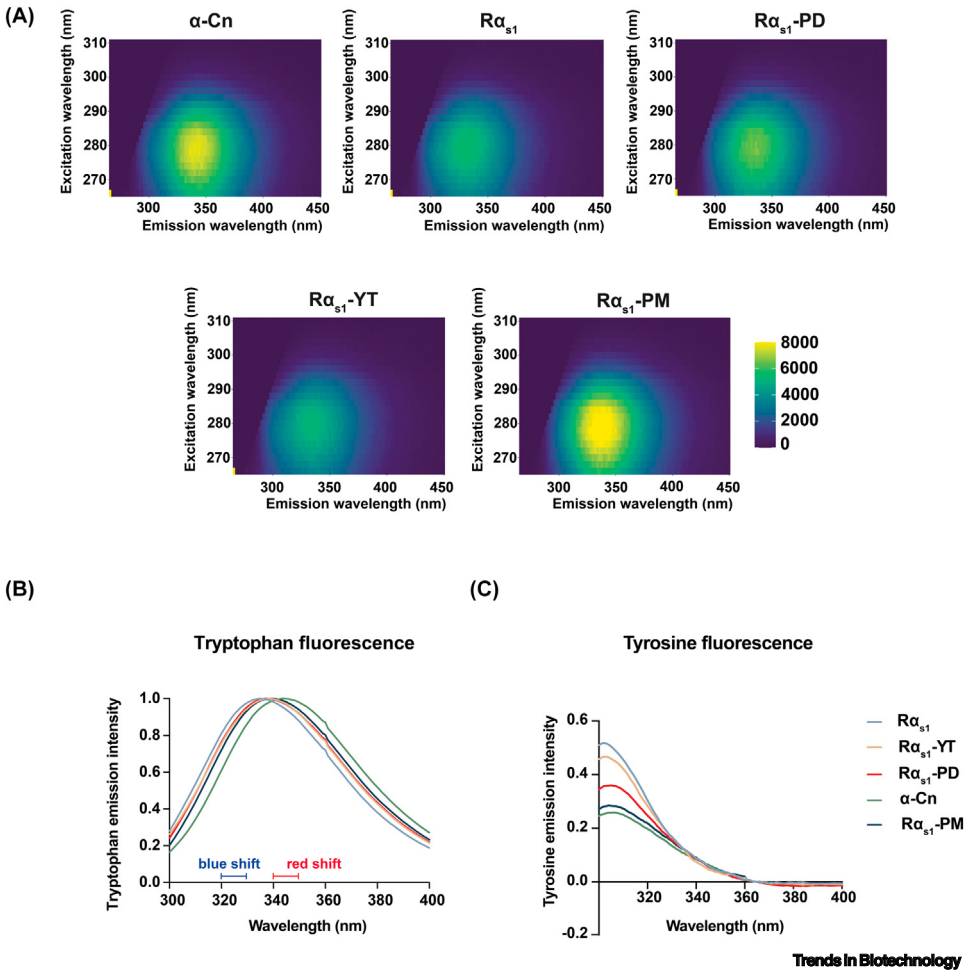

Figure 5. Structural characterization of bovine α-casein, *in vivo* phosphorylated and phosphomimetic α_{s1}-casein. 2D and 3D-fluorescence spectroscopic analyses: (A) 3D fluorescence spectra were recorded with excitation range 210–495 nm and an emission range 230–520 nm, at 700 V. (B) Emission spectra of recombinant α_{s1}-caseins at 290 nm, highlighting tryptophan contributions. Fluorescence intensities were normalized to the maximum value of the data set. (C) Emission spectra of recombinant α_{s1}-casein at 275 nm, highlighting tyrosine contributions. α-casein (α-cn) was used as a positive control.

303–310 nm) as the primary fluorophores with varying intensities. The 2D analysis further revealed distinct emission maxima (λ_{max}) across samples, indicating structural differences. α-casein, with its λ_{max} of 344 nm, indicated that Trp is exposed to polar solvent, suggesting an expanded conformation in the vicinity of Trp. By contrast, the phosphorylated/phosphomimetic α_{s1}-caseins, Rα$_{s1}$-PD, Rα$_{s1}$-YT, and Rα$_{s1}$-PM, exhibited a shift toward lower wavelengths (~338/339 nm), suggesting that the local environment of Trp is in limited contact with water. The shift was even more pronounced for the unphosphorylated Rα$_{s1}$, which exhibited a λ_{max} of 335 nm, suggesting that Trp is close to nonpolar regions of the protein [66]. The observed changes in the Trp fluorescence environment likely reflect alterations in protein conformation and/or oligomerization state.

Considering that α-casein is intrinsically disordered, it is unlikely that the absence of phosphorylation induces folding. This hypothesis is further supported by circular dichroism (CD) data indicating

a low secondary structure content (data not shown). Therefore, the observed shifts in fluorescence maxima are likely due to changes in oligomerization state, which modify the local environment of Trp residues. Phosphorylation is known to affect charge distribution, hydrophilicity, and intermolecular interactions [29], all of which could impact self-assembly and oligomer formation.

To further assess oligomerization tendencies, recombinant α_{s1}-caseins were analyzed using dynamic light scattering (DLS) to determine their hydrodynamic radii and aggregation states. DLS measurements (Figure S2 in the supplemental information online) revealed that bovine α-casein and unphosphorylated Rα_{s1}-casein had the smallest hydrodynamic diameter, ~6 nm, while the phosphorylated α_{s1}-caseins - Rα_{s1}-PD, Rα_{s1}-YT, and Rα_{s1}-PM displayed larger diameters, ~12 nm. No large aggregates were detected, suggesting that Rα_{s1}-PD, Rα_{s1}-YT, and Rα_{s1}-PM remained in a generally low aggregation state with good solubility.

Discussion

The increasing demand for sustainable alternatives to traditional dairy proteins has driven interest in precision fermentation and recombinant casein production. Traditional dairy farming is under pressure to reduce its environmental footprint, particularly regarding methane emissions, water use, and land consumption. In this context, microbial production of caseins via recombinant expression systems offers a promising alternative by reducing reliance on livestock while maintaining the functional properties necessary for dairy applications. Precision fermentation of milk proteins have emerged as a key focus area, aiming to replicate native dairy protein functionality without animal-derived sources. However, for this approach to be commercially viable, scalability and efficiency of microbial protein production must be considered. While this study primarily serves as a proof of concept, demonstrating that microbial cell factories can produce recombinant caseins with biologically relevant phosphorylation patterns, the potential for industrial-scale production is an important factor in determining its feasibility.

Literature suggests that high cell-density fermentation in *E. coli* can yield up to 9.7 g/l of recombinant protein, a level that may be sufficient for commercial applications [67–70]. However, *E. coli* presents challenges in protein secretion, necessitating intracellular accumulation and complex purification steps. Alternative microbial hosts, such as *Bacillus* spp, *Aspergillus* spp, *Saccharomyces* spp, and *Komagataella* spp, offer potential advantages in terms of secretion efficiency and downstream processing, further supporting the feasibility of scaling up recombinant casein production. Economic modelling studies have also highlighted the commercial viability of producing recombinant milk proteins using yeast and bacterial systems, reinforcing the long-term potential of this approach [71,72].

This study explores two approaches for producing functional recombinant caseins: phosphomimetic modification and kinase co-expression systems. The phosphomimetic strategy offers a simpler production setup, eliminating the need for kinase co-expression, reducing metabolic burden and potentially increasing expression yields. In this work, phosphomimetic modifications demonstrated an ability to mimic casein structure and function to a considerable extent, suggesting their potential for food applications. Rα_{s1}-PM exhibited calcium-binding capacity comparable to the control, with only a slight but statistically significant difference. However, it remains unclear whether phosphomimetic modifications can fully replicate the role of casein in micelle formation, particularly in sequestering amorphous calcium phosphate into stable nanoclusters.

By contrast the kinase co-expression system offers tunability in phosphorylation levels, allowing precise control over casein phosphorylation by modulating bacterial kinase expression. This is particularly important for tailoring micelle size and stability, which influence gel network formation

in food matrices [43]. While mammalian kinases, such as Fam20C, are challenging to express in microbial hosts, bacterial kinases, such as PrkD and YabT, from *B. subtilis* offer a simpler and more accessible alternative due to their ease of expression. However, their broader substrate specificity led to phosphorylation of few non-native sites, which may influence casein self-assembly and functional properties.

MS analysis confirmed that *in vitro* phosphorylated recombinant caseins mimic native bovine casein phosphorylation sites, while 2DE and phospho-staining qualitatively validated *in vivo* phosphorylation. Furthermore, the results demonstrated that phosphorylation significantly enhanced calcium binding, a key function of caseins. It is well-established that three or more SerP residues within a short peptide sequence form a PC, essential for binding calcium ions and stabilizing calcium phosphate nanoclusters [37,73–75]. Given that bacterial kinase effectively phosphorylated all the potential seryl residues, it is likely that these recombinant phosphopeptides contain PCs capable of binding calcium ions. However, whether these phosphorylated recombinant α_{s1}-caseins contain a considerable number of PCs to sequester amorphous calcium phosphate and form stable nanoclusters remains an open question, requiring further validation in future studies.

Beyond functional effects, phosphorylation and phosphomimetic modifications appear to modulate casein structure and oligomerization. The fluorescence intensity of Trp and Tyr vary across the different recombinant α_{s1}-caseins. Phosphorylation and phosphomimetic modifications likely influence local structural dynamics, which, in turn, may affect energy transfer between Tyr and Trp residues. Given that Tyr-to-Trp fluorescence resonance energy transfer (FRET) depends on both distance and orientation [76], these modifications might alter the spectral properties in a way that influences the apparent fluorescence yield of Trp179. In addition, the phosphorylated Tyr may introduce new electrostatic interactions that perturb local solvation or alter the overall conformation of the protein, contributing to the differences in fluorescence emission [77]. Consistent with this, CD analysis confirms that these changes occur without inducing significant folding, instead suggesting subtle conformational rearrangements and differences in oligomerization. These conformational changes, together with the observed differences in hydrodynamic radius, indicate phosphomimetic/phosphorylation-dependent changes in oligomerization. These modification-induced structural changes, particularly near Trp179, could alter its local environment and contribute to the observed spectral shifts. Further studies using size-exclusion chromatography coupled with multi-angle light scattering would provide additional quantitative insights into the oligomerization state. Despite the need for more quantitative analysis, the current evidence already points toward a coherent picture. The approaches established in this study lay scientific groundwork toward the longstanding goal of harnessing microbial production of caseins for future dairy and food applications.

Concluding remarks

The market share of animal-derived products in 2040 is projected to significantly decrease compared with current levels. Over the coming years, the market will diversify, with nutritionally and functionally equivalent or superior plant-based or precision fermentation-based alternatives widely adopted by consumers in their daily diets. We propose that recombinant caseins, such as those presented here, can have a pivotal role in realizing this vision.

The ability to produce phosphorylated recombinant caseins represents a transformative breakthrough in the alternative protein industry, addressing the longstanding challenge of achieving phosphorylation at native sites, a key barrier to commercialization. By refining phosphorylation strategies, this work lays the foundation for producing functional recombinant caseins. Future studies should extend to other casein proteins while focusing on optimizing secretion efficiency,

Outstanding questions

Can these strategies be adapted across other casein types (e.g., α_{s2}, β-, and κ-casein)?

Do bacterial kinases exhibit sufficient substrate flexibility to phosphorylate other structurally diverse proteins used in food or biopharmaceutical applications?

Can microbial production of phosphorylated caseins achieve cost parity or superiority over bovine-derived caseins at scale?

Can recombinant caseins phosphorylated by bacterial kinases form calcium phosphate nanoclusters, thereby enabling micelle formation and stabilization similar to native bovine caseins?

To what extent can phosphomimetic modifications replicate the biophysical and functional roles of phosphate groups in micelle stabilization and calcium phosphate nanocluster formation?

enhancing kinase specificity, and validating the formation of stable calcium phosphate nanoclusters (see Outstanding questions). These advances will be essential for scaling up recombinant casein production and facilitating their integration into sustainable, animal-free dairy applications.

STAR★METHODS

Detailed methods are provided in the online version of this paper and include the following:

- KEY RESOURCES TABLE
- EXPERIMENTAL MODEL AND STUDY PARTICIPANT DETAILS
- METHOD DETAILS
  - Synthetic genes and DNA
  - Media
  - Plasmid and strain construction
  - Protein production
  - *In vitro* phosphorylation of caseins
  - 1- and 2-D gel electrophoresis
  - Sample preparation for liquid chromatography mass spectrometry (LC-MS)
  - LC-MS analysis of *in vitro* phosphorylated proteins
  - Analysis of proteomics data
  - *In vitro* digestion of recombinant α_{s1}-casein
  - Calcium binding assay
  - Fluorescence spectroscopy
  - Particle size and electrophoretic mobility measurements
- QUANTIFICATION AND STATISTICAL ANALYSIS

RESOURCE AVAILABILITY

Lead contact

Requests for further information and resources should be directed to, and will be fulfilled by the lead contact, Ivan Mijakovic (ivan.mijakovic@chalmers.se).

Materials availability

All the strains generated in this study will be made available on request for non-commercial research purposes and will require a materials transfer agreement.

Data and code availability

Mass spectrometry data are available via ProteomeXchange with identifier PXD057429 and are publicly available as of the date of publication.

Author contributions

P.R.J., I.M., and S.B. conceived the study. P.R.J. and I.M. supervised the study. S.B. performed the strain construction, protein production, *in vivo* phosphorylation, and 2DE. G.M. performed *in vitro* phosphorylation. S.B. and G.M. performed the *in vitro* digestion and calcium-binding assays. J.B.K. ran LC-MS for identification of the phospho-sites. S.B. performed DLS, 2D and 3D fluorescence spectroscopy under the supervision of A.B. and C.B.C. S.B. and I.M. wrote the original draft. S.B. revised the draft. All the authors edited the paper and approved the final version.

Acknowledgments

We would like to thank Rune Busk Damgaard, and Julian Koch for providing access to the ChemiDoc MP system. We would like to thank Joëlle Davy for her technical support during fluorescence spectroscopy analysis. We acknowledge funding from the Swedish Research Council (Vetenskapsrådet grant number 391 2020-03176), the Novo Nordisk Foundation (grant number NNF20CC0035580) to I.M., and the Novo Nordisk Foundation (grant number NNF21OC0071334) to I.M. and P.R.J.

Declaration of interests

S.B., P.R.J., C.J., G.M., I.M., and L.S. are co-inventors on a patent application related to this study. The other authors declare no competing interests.

Supplemental information

Supplemental information associated with this article can be found online at https://doi.org/10.1016/j.tibtech.2025.05.015.

References

1. Lajnaf, R. *et al.* (2022) Promising food ingredients: milk proteins. In *Bovine Science - Challenges and Advances* (Abubakar, M., ed.), pp. 99092, IntechOpen
2. Balivo, A. *et al.* (2024) Sensory properties of foods functionalised with milk proteins. *Food Hydrocoll.* 147, 109301
3. Livney, Y.D. (2010) Milk proteins as vehicles for bioactives. *Curr. Opin. Colloid Interface Sci.* 15, 73–83
4. Berry, S. *et al.* (2020) Defining the origin and function of bovine milk proteins through genomics: the biological implications of manipulation and modification. In *Milk Proteins* (Boland, M. and Singh, H., eds), pp. 143–171, Elsevier
5. Bava, L. *et al.* (2014) How can farming intensification affect the environmental impact of milk production? *J. Dairy Sci.* 97, 4579–4593
6. Castanheira, É.G. *et al.* (2010) The environmental performance of milk production on a typical Portuguese dairy farm. *Agric. Syst.* 103, 498–507
7. Future Market Insights (2025) *Casein Market - Increasing Adoption of Dairy Proteins in Emerging Economies Is Shaping Casein Market. 2023-2033*, Future Market Insights
8. Abd El-Salam, M.H. and El-Shibiny, S. (2017) Preparation, properties, and uses of enzymatic milk protein hydrolysates. *Crit. Rev. Food Sci. Nutr.* 57, 1119–1132
9. Elzoghby, A.O. *et al.* (2011) Casein-based formulations as promising controlled release drug delivery systems. *J. Control. Release* 153, 206–216
10. Verstraete, W. and De Vrieze, J. (2017) Microbial technology with major potentials for the urgent environmental needs of the next decades. *Microb. Biotechnol.* 10, 988–994
11. Graham, A.E. and Ledesma-Amaro, R. (2023) The microbial food revolution. *Nat. Commun.* 14, 2231
12. Knychala, M.M. *et al.* (2024) Precision fermentation as an alternative to animal protein, a review. *Fermentation* 10, 315
13. Matassa, S. *et al.* (2016) Microbial protein: future sustainable food supply route with low environmental footprint. *Microb. Biotechnol.* 9, 568–575
14. Lagassé, H.A.D. *et al.* (2017) Recent advances in (therapeutic protein) drug development. *F1000Res* 6, 113
15. Gelli, H.P. *et al.* (2025) Enhancing intestinal absorption of a macromolecule through engineered probiotic yeast in the murine gastrointestinal tract. *Trends Biotechnol.* 43, 715–731
16. Li, C. *et al.* (2020) Developing *Aspergillus niger* as a cell factory for food enzyme production. *Biotechnol. Adv.* 44, 107630
17. Balasubramanian, S. *et al.* (2024) Exploring the secretome of *Corynebacterium glutamicum* ATCC 13032. *Front. Bioeng. Biotechnol.* 12, 1348184
18. Mridul, A. (2024) Unilever to Launch Breyers Ice Cream with Perfect Day's Precision-Fermented Whey. *Green Queen*, Published online February 23, 2024. https://www.greenqueen.com.hk/unilever-breyers-lactose-free-ice-cream-perfect-day-precision-fermentation/
19. Scipioni, J. (2019) This $20 Ice Cream Is Made with Dairy Grown in Lab—and It Sold Out Immediately. Published on line July 16, 2019. https://www.cnbc.com/2019/07/16/perfect-day-foods-made-ice-cream-from-real-dairy-grown-in-lab.html
20. Straughn, S. (2022) Animal-free dairy grows in popularity with consumers. *Supermarket Perimeter*, Published online July 25, 2022. https://www.supermarketperimeter.com/articles/8455-animal-free-dairy-grows-in-popularity-with-consumers
21. Kalidas, C. *et al.* (2001) Characterization of glycosylated variants of β-lactoglobulin expressed in *Pichia pastoris*. *Protein Eng. Des. Sel.* 14, 201–207
22. Jia, B. and Jeon, C.O. (2016) High-throughput recombinant protein expression in *Escherichia coli* : current status and future perspectives. *Open Biol.* 6, 160196
23. Saito, A. *et al.* (2002) Secretion of glycosylated alpha-lactalbumin in yeast *Pichia pastoris*. *J. Biochem.* 132, 77–82
24. Choi, B.-K. and Jiménez-Flores, R. (2001) Expression and purification of glycosylated bovine β-casein (L70S/P71S) in *Pichia pastoris*. *J. Agric. Food Chem.* 49, 1761–1766
25. Corredig, M. and Dalgleish, D.G. (1997) Studies on the susceptibility of membrane-derived proteins to proteolysis as related to changes in their emulsifying properties. *Food Res. Int.* 30, 689–697
26. Lima Nascimento, L.G. *et al.* (2023) Combination of milk and plant proteins to develop novel food systems: what are the limits? *Foods* 12, 2385
27. Yang, Y. *et al.* (2024) Casein-based hydrogels: advances and prospects. *Food Chem.* 447, 138956
28. Uversky, V.N. and Kulkarni, P. (2021) Intrinsically disordered proteins: chronology of a discovery. *Biophys. Chem.* 279, 106694
29. Holt, C. *et al.* (2013) Caseins and the casein micelle: their biological functions, structures, and behavior in foods. *J. Dairy Sci.* 96, 6127–6146
30. Redwan, E. *et al.* (2015) Disorder in milk proteins: caseins, intrinsically disordered colloids. *Curr. Protein Pept. Sci.* 16, 228–242
31. Schneider, R. *et al.* (2019) Experimental studies of binding of intrinsically disordered proteins to their partners. In *Intrinsically Disordered Proteins* (Salvi, N., ed.), pp. 139–187, Elsevier
32. Gagnaire, V. *et al.* (1996) Phosphopeptides interacting with colloidal calcium phosphate isolated by tryptic hydrolysis of bovine casein micelles. *J. Dairy Res.* 63, 405–422
33. Aoki, T. *et al.* (1986) Separation of casein aggregates cross-linked by colloidal calcium phosphate from bovine casein micelles by high performance gel chromatography in the presence of urea. *J. Dairy Res.* 53, 53–59
34. Aoki, T. *et al.* (1987) Caseins are cross-linked through their ester phosphate groups by colloidal calcium phosphate. *Biochim. Biophys. Acta Protein Struct. Mol. Enzymol.* 911, 238–243
35. Azuma, N. *et al.* (1989) Effect of bound phosphate on the calcium-binding ability and calcium-dependent precipitability of human β-casein. *Agric. Biol. Chem.* 53, 1037–1041
36. Baumy, J.-J. *et al.* (1989) Study of calcium binding to phosphoserine residues of β -casein and its phosphopeptide (1–25) by ^{31}P NMR. *J. Dairy Res.* 56, 403–409
37. Aoki, T. *et al.* (1992) The least number of phosphate groups for crosslinking of casein by colloidal calcium phosphate. *J. Dairy Sci.* 75, 971–975
38. Holt, C. *et al.* (2009) Role of calcium phosphate nanoclusters in the control of calcification. *FEBS J.* 276, 2308–2323
39. De Kruif, C.G. and Holt, C. (2003) Casein micelle structure, functions and interactions. In *Advanced Dairy Chemistry—1 Proteins* (Fox, P.F. and McSweeney, P.L.H., eds), pp. 233–276, Springer
40. Dalgleish, D.G. (1993) The enzymatic coagulation of milk. In *Cheese: Chemistry, Physics and Microbiology* (Fox, P.F., ed.), pp. 69–100, Springer
41. Choi, J. *et al.* (2008) Effects of the concentration of insoluble calcium phosphate associated with casein micelles on the functionality of directly acidified cheese. *J. Dairy Sci.* 91, 513–522
42. Che, J. *et al.* (2025) Unravelling the dominant role of phosphorylation degree in governing the functionality of reassembled casein micelles: implications for future dairy production through precision fermentation. *Food Hydrocoll.* 159, 110615
43. Antuma, L.J. *et al.* (2023) Engineering artificial casein micelles for future food: Is casein phosphorylation necessary? *Food Res. Int.* 173, 113315
44. Raynes, J.K. *et al.* (2024) Structure of biomimetic casein micelles: critical tests of the hydrophobic colloid and multivalent-binding models using recombinant deuterated and phosphorylated β-casein. *J. Struct. Biol. X* 9, 100096
45. Clegg, R.A. *et al.* (2009) *coli* over-expression system for multiply-phosphorylated proteins and its use in a study of calcium phosphate sequestration by novel recombinant phosphopeptides. *Protein Expr. Purif.* 67, 23–34
46. Bijl, E. *et al.* (2014) Phosphorylation of αS1-casein is regulated by different genes. *J. Dairy Sci.* 97, 7240–7246
47. Tagliabracci, V.S. *et al.* (2015) A single kinase generates the majority of the secreted phosphoproteome. *Cell* 161, 1619–1632

48. Tagliabracci, V.S. *et al.* (2012) Secreted kinase phosphorylates extracellular proteins that regulate biomineralization. *Science* 1979, 1150–1153
49. Mijakovic, I. *et al.* (2016) Exploring the diversity of protein modifications: special bacterial phosphorylation systems. *FEMS Microbiol. Rev.* 40, 398–417
50. Stancik, I.A. *et al.* (2018) Serine/threonine protein kinases from Bacteria, Archaea and Eukarya share a common evolutionary origin deeply rooted in the Tree of Life. *J. Mol. Biol.* 430, 27–32
51. Jers, C. *et al.* (2011) *Bacillus subtilis* two-component system sensory kinase DegS is regulated by serine phosphorylation in its input domain. *PLoS ONE* 6, e14653
52. Nagao, M. *et al.* (1988) Expression of bovine α_{s1} -casein cDNA in *Escherichia coli*. *Agric. Biol. Chem.* 52, 191–200
53. Schulmeister, U. *et al.* (2009) Cloning, expression, and mapping of allergenic determinants of αS1-casein, a major cow's milk allergen. *J. Immunol.* 182, 7019–7029
54. Fang, Z.H. *et al.* (2016) The relationships among bovine αS-casein phosphorylation isoforms suggest different phosphorylation pathways. *J. Dairy Sci.* 99, 8168–8177
55. Farrell, H.M. *et al.* (2004) Nomenclature of the proteins of cows' milk—sixth revision. *J. Dairy Sci.* 87, 1641–1674
56. Dzhanaev, R. *et al.* (2023) Application of the mineral-binding protein fetuin-A for the detection of calcified lesions. *Theranostics* 13, 659–672
57. Léger, J. *et al.* (1997) Conversion of serine to aspartate imitates phosphorylation-induced changes in the structure and function of microtubule-associated protein Tau. *J. Biol. Chem.* 272, 8441–8446
58. Brodkorb, A. *et al.* (2019) INFOGEST static in vitro simulation of gastrointestinal food digestion. *Nat. Protoc.* 14, 991–1014
59. Dupont, D. *et al.* (2010) Comparative resistance of food proteins to adult and infant *in vitro* digestion models. *Mol. Nutr. Food Res.* 54, 767–780
60. Tang, N. and Skibsted, L.H. (2016) Calcium binding to amino acids and small glycine peptides in aqueous solution: toward peptide design for better calcium bioavailability. *J. Agric. Food Chem.* 64, 4376–4389
61. Jiang, Y. *et al.* (2021) Binding of calcium to l-serine and o-phospho-l-serine as affected by temperature, pH and ionic strength under milk processing conditions. *Int. Dairy J.* 112, 104875
62. Hiraoka, Y. *et al.* (1980) α-Lactalbumin: a calcium metalloprotein. *Biochem. Biophys. Res. Commun.* 95, 1098–1104
63. Permyakov, E.A. (2020) α-Lactalbumin, amazing calcium-binding protein. *Biomolecules* 10, 1210
64. Hinderink, E.B.A. *et al.* (2021) Conformational changes of whey and pea proteins upon emulsification approached by front-surface fluorescence. *J. Agric. Food Chem.* 69, 6601–6612
65. Dalgleish, D.G. (1973) A study of the interaction of calcium ions with bovine α_{s1} -casein using fluorescence spectroscopy. *Eur. J. Biochem.* 40, 375–380
66. Burstein, E.A. *et al.* (1973) Fluorescence and the location of tryptophan residues in protein molecules. *Photochem. Photobiol.* 18, 263–279
67. Jeong, K.J. *et al.* (2004) Constitutive production of human leptin by fed-batch culture of recombinant rpoS– *Escherichia coli*. *Protein Expr. Purif.* 36, 150–156
68. Choi, J.H. *et al.* (2003) Enhanced production of insulin-like growth factor I fusion protein in *Escherichia coli* by coexpression of the down-regulated genes identified by transcriptome profiling. *Appl. Environ. Microbiol.* 69, 4737–4742
69. Vallejo, L.F. *et al.* (2002) Renaturation and purification of bone morphogenetic protein-2 produced as inclusion bodies in high-cell-density cultures of recombinant *Escherichia coli*. *J. Biotechnol.* 94, 185–194
70. Shin, C.S. *et al.* (1997) Enhanced production of human mini-proinsulin in fed-batch cultures at high cell density of *Escherichia coli* BL21(DE3)[pET-3aT2M2]. *Biotechnol. Prog.* 13, 249–257
71. Vestergaard, M. *et al.* (2016) Can microbes compete with cows for sustainable protein production - a feasibility study on high quality protein. *Sci. Rep.* 6, 36421
72. Deng, M. *et al.* (2023) Cell factory-based milk protein biomanufacturing: advances and perspectives. *Int. J. Biol. Macromol.* 244, 125335
73. Holt, C. *et al.* (1996) Ability of a β -casein phosphopeptide to modulate the precipitation of calcium phosphate by forming amorphous dicalcium phosphate nanoclusters. *Biochem. J.* 314, 1035–1039
74. West, D.W. (1986) Structure and function of the phosphorylated residues of casein. *J. Dairy Res.* 53, 333–352
75. Lenton, S. *et al.* (2015) A review of the biology of calcium phosphate sequestration with special reference to milk. *Dairy Sci. Technol.* 95, 3–14
76. Davis, K.B. *et al.* (2018) Application of tyrosine-tryptophan fluorescence resonance energy transfer in monitoring protein size changes. *Anal. Biochem.* 557, 142–150
77. Hunter, T. (2014) The genesis of tyrosine phosphorylation. *Cold Spring Harb. Perspect. Biol.* 6, a020644
78. Shi, L. *et al.* (2014) Cross-phosphorylation of bacterial serine/threonine and tyrosine protein kinases on key regulatory residues. *Front. Microbiol.* 5, 495
79. Amrein, K.E. *et al.* (1995) Purification and characterization of recombinant human p50csk protein-tyrosine kinase from an *Escherichia coli* expression system overproducing the bacterial chaperones GroES and GroEL. *Proc. Natl. Acad. Sci. U. S. A.* 92, 1048–1052
80. Cao, Y. *et al.* (2017) Bioactive peptides isolated from casein phosphopeptides enhance calcium and magnesium uptake in Caco-2 cell monolayers. *J. Agric. Food Chem.* 65, 2307–2314

STAR★METHODS

KEY RESOURCES TABLE

Reagent or resource	Source	Identifier
Bacterial and virus strains		
Escherichia coli BL21(DE3)	Lab stock	N/A
Escherichia coli TOP10	Thermo Fisher Scientific	404010
Escherichia coli M15	Lab stock	N/A
Chemicals, peptides, and recombinant proteins		
Ampicillin	Sigma Aldrich	A0166
Kanamycin	Sigma Aldrich	K1377
IPTG	AG Scientific	I-1312
InstantStain	Kem En Tec	INST-1L-181
Lysogeny broth (Miller)	Sigma Aldrich	L3522
Lysogeny broth (Lennox) agar	Sigma Aldrich	L2897
Sodium chloride	Sigma-Aldrich	S9888
Glycerol	VWR chemicals	23B214119
Imidazole	Sigma-Aldrich	56750
Urea	Sigma-Aldrich	U5378
MOPS	Sigma-Aldrich	M3981
CHAPS	Sigma-Aldrich	850500P
4x Laemmli sample buffer	Bio-Rad	1610747
Bio-lyte	Bio-Rad	1632094
4–20% Criterion™ Tris-HCl Protein Gel, 11 cm IPG/prep+1 well, 550 µl	Bio-Rad	3450104
ReadyStrip™ IPG Strips; 11 cm, pH 4–7	Bio-Rad	1632015
4–20% Mini-PROTEAN® TGX™ Precast Gel	Bio-Rad	4561096EDU
10x Tris/Glycine/SDS	Bio-Rad	1610732
SDS	Sigma-Aldrich	L3771
Iodoacetamide	Sigma-Aldrich	I6125
DTT	Sigma-Aldrich	D5545
Trypsin/Lys-C	Promega	V5071
Pancreatin	Sigma-Aldrich	P7545
Bile	Sigma-Aldrich	B3883
Pepsin	Roche	10108057001
Simulated intestinal fluid	Biochemazone	BZ176
Simulated gastric fluid	Biochemazone	BZ175
Artificial human saliva	Biochemazone	BZ323
Sodium hydroxide	Sigma-Aldrich	S5881
FastAP	Thermo Fisher Scientific	EF0651
Methanol	Supelco	I1285012
Precision Plus Protein Dual Color Standards	Bio-Rad	1610374
Peppermintstick phosphoprotein	Thermo Fisher Scientific	P27167
Formic acid	Sigma-Aldrich	822254

(continued)

Reagent or resource	Source	Identifier
Acetonitrile	Sigma-Aldrich	34851
Potassium chloride	Sigma-Aldrich	P3911
Magnesium chloride	Sigma-Aldrich	M8266
Triton X-100	Sigma-Aldrich	X100
Bovine serum albumin	Sigma-Aldrich	05470
Bovine α-casein	Sigma-Aldrich	C6780
Trizma	Sigma-Aldrich	T1503
Pro-Q diamond phosphoprotein gel stain	Thermo Fisher Scientific	MP 33300
SYPRO RUBY total protein stain	Thermo Fisher Scientific	S12000
Mineral oil	Bio-Rad	1632129
Low melt agarose	Bio-Rad	1613111
Acetic acid	Sigma-Aldrich	33209
Bromophenol blue	Sigma-Aldrich	318744
Tween-20	Sigma-Aldrich	P1379
Critical commercial assays		
Calcium Colorimetric Assay Kit	Sigma-Aldrich	MAK022
Deposited data		
LC-MS/MS data	ProteomeXchange	PXD057429
Oligonucleotides		
Primers	IDT	Table S2 in the supplemental information online
Recombinant DNA		
Genes	IDT	Table S1 in the supplemental information online
Software and algorithms		
SpectronautTM (Version 17.1)		https://biognosys.com/software/spectronaut/
Snapgene		https://www.snapgene.com/
GraphPad Prism (Version 10)		https://www.graphpad.com/
RStudio		https://posit.co/download/rstudio-desktop/
Adobe illustrator 2025		https://www.adobe.com/products/illustrator.html
Biorender.com		https://www.biorender.com/

EXPERIMENTAL MODEL AND STUDY PARTICIPANT DETAILS

All *Escherichia coli* (*E. coli*) strains producing α_{s1}-caseins, and casein-kinase fusions were generated from *E. coli* BL21(DE3). For bacterial kinase production, *E. coli* M15 strain was used. For cloning, *E. coli* Top10 was used.

METHOD DETAILS

Synthetic genes and DNA

Heterologous genes of α_{s1}-casein (16-214), α_{s1}-casein-PM (16-214, substituted with aspartic acid), and Fam20Cs were synthesized (Genscript and IDT respectively) and codon optimized for *E. coli* using the codon-optimization tool provided by their respective companies. The sequences can be found in the Table S1 in the supplemental information online. Oligonucleotides for PCR for synthesizing genes from the genome of *B. subtilis* were obtained from IDT and are listed in the Table S2 in the supplemental information online.

Media

Standard lysogeny broth (LB, 10 g/L tryptone, 5 g/L yeast extract, 5 g/L NaCl, which was solidified with/without 1.5% agar as necessary) from Sigma-Aldrich supplemented with appropriate antibiotics was used for the growth and cultivation of the bacterial strains. Isopropyl β-D-thiogalactoside (IPTG) from AG Scientific was used as an inducer for facilitating protein expression.

For sonication and purification, native buffers containing 20 mM MOPS, 100 mM NaCl, and Imidazole (20 mM for binding, and 500 mM for elution) were used.

Plasmid and strain construction

α_{s1}-casein gene with relevant restriction sites was inserted downstream of the 6xHis-tag in the pET15b vector, which was digested with NdeI and BamHI (pET15b_As1).

Three prokaryotic Hanks-type serine/threonine kinases from *Bacillus subtilis* (PrkC, PrkD, YabT), and two eukaryotic serine/threonine kinases, Fam20C from human (Hf20C), and bovine (Bf20C) were chosen for *in vitro* phosphorylation. For Fam20Cs, Gibson compatible genes were synthesized by IDT and inserted downstream of the 6xHis-tag in the pET15b vector, which was digested with NdeI and BamHI (pET15b_Bf20C, and pET15b_Hf20C). The three kinases from *B. subtilis* PrkC, PrkD, and YabT were previously constructed using pQE-30 by Shi and colleagues (2014) [78] (will be called as pQE-30_PrkC, pQE-30_PrkD, and pQE-30_YabT respectively).

For phosphomimetic modification, all eight phosphoserine sites (α_{s1}-casein, Variant B) were substituted by aspartic acid and synthesized as a Gibson compatible gblock fragment from IDT. The gene was inserted downstream of the 6xHis-tag in the pET15b vector, which was digested with NdeI and BamHI (pET15b_As1-Asp).

For facilitating, *in vivo* phosphorylation, Gibson compatible PCR products containing RBS and X kinase (PrkD/YabT) were generated from pQE-30_PrkD, and pQE-30_YabT, were inserted into pET15b_As1 linearized by PCR. This resulted in α_{s1}-casein and X kinase (PrkD/YabT) in tandem under the control of T7 promoter. All the protein and primer sequences can be found in the supplementary information.

All the strains containing constructs with either a phosphomimetic casein or a kinase were transformed with pREP4 plasmid containing the chaperonins GroEL/GroES (pREP4_GroES/EL) to assist with folding and solubility [79]. All the transformants were selected on LB agar supplemented with appropriate antibiotics (ampicillin 100 µg/ml for pET15B and pQE-30, and kanamycin 25 µg/ml for pREP4) [25].

Protein production

Protein synthesis and purification were conducted as described previously [78]. In brief, cells were grown at 37 °C, 200 rpm until late-exponential phase (OD_{600} =0.8) and induced with 0.5 mM IPTG at 30 °C, 200 rpm and harvested after 16 hours at 13000 g for 20 minutes. The cells were lysed in native binding buffer (20 mM phosphate buffer, 500 mM NaCl, 50 mM Imidazole, 5% glycerol, pH 7.4) with protease inhibitor, 1 mg/ml lysozyme by sonication (10 second on and 15 second off cycle, 20 minutes). The cells were kept on ice throughout the process to prevent degradation. The His-tag proteins were purified from the lysate by affinity chromatography using HISTRAP FF CRUDE column in ÄKTA Pure 25M (Cytiva). To elute the His-tagged proteins, elution buffer (20 mM phosphate buffer, 500 mM NaCl, 500 mM Imidazole, 5% glycerol, pH 7.4) was used.

In vitro phosphorylation of caseins

Protein samples were desalted using PD-10 columns (Cytiva) and stored in 10% glycerol prior to *in vitro* phosphorylation. *In vitro* protein phosphorylation experiments were conducted using 3 µM of kinases (PrkD (30 kDa), PrkC (40 kDa), and YabT (35.7 kDa)) and 15 µM of target protein (α_{s1} (24 kDa)). Each 35 µl reaction mixture also contained 50 µM of [γ-32P]-ATP (20 µCi/mmol), 50 µM ATP, 5 mM MgCl2, 100 mM NaCl, 5% glycerol and 50 mM Tris–HCl pH 7.5. Following a 1-hour incubation at 37 °C, the reactions were stopped by adding sample buffer for SDS–PAGE and heating at 100 °C for 5 minutes. Electrophoresis was performed on 8-12% SDS-polyacrylamide gels (Bio-Rad), which were subsequently treated with boiling 0.5 M HCl for 10 minutes. The gels were then dried by Gel-Dry™ Drying Solution (Invitrogen), and radioactive bands were visualized by Amersham TYPHOON™ scanner (Amersham typhoon control software version 3.0.0.2, firmware version 303, Cytiva Life Science) after an exposure time of 24 hours.

1- and 2-D gel electrophoresis

For 1-DE protein separation by SDS-PAGE, 10 µL of cell lysate was mixed with 4x Laemmli sample buffer containing 100 mM DTT and boiled at 95°C for 5 minutes. The protein samples were then loaded onto and separated on a precast 4-20% Tris-glycine criterion gel (Bio-Rad). The gels were stained with InstantStain Coomasie Stain and visualized on ChemiDoc XRS.

For isoelectric focusing (IEF), 11 cm pH 4-7 IPG strips (Bio-Rad) were used with the IPGPhor system (Amersham). The strips were rehydrated for 6 h with 200 µL of rehydration buffer containing 50 µg of protein, 8 M urea, 2% CHAPS, 2% Bio-Lyte, and 50 mM DTT. During rehydration, the strips were covered with 300 µL of mineral oil. After rehydration, isoelectric focusing was conducted using a series of voltage steps. First, a step-and-hold phase was applied at 500 V for 1 hour, reaching a total of 0.5 kVh. This was followed by a gradient increase to 1000 V over the next hour. The voltage was then further increased with a gradient up to 6000 V for 2.5 hours. Finally, a step-and-hold phase at 6000 V was maintained for 50 minutes.

Following isoelectric focusing, the IPG strips were equilibrated sequentially in two distinct buffers. The first equilibration buffer (Buffer I) contained 6 M urea, 30% (w/v) glycerol, 2% (w/v) SDS, 0.05 M Tris-HCl (pH 8.8), and 1% DTT, and the strips were incubated in this solution for 10 minutes. In the second equilibration buffer (Buffer II), the composition was the same as Buffer I, except 4% iodoacetamide replaced DTT; the strips were also incubated in this buffer for 10 minutes. After equilibration, the strips were rinsed with the running buffer to prepare for subsequent analysis.

The equilibrated IPG strips were placed onto the precast 4-20% Tris-HCl criterion gel (Bio-Rad), with the gel side facing up. A wick soaked in 4 µL of peppermint phosphoprotein ladder was placed alongside the strip, and both were sealed with 0.1% low-melting agarose. The gel was run at 180 V for 60 minutes.

The gel was stained first with Pro-Q Diamond for phosphoproteins and then with SYPRO Ruby for total protein detection, following the manufacturer's protocols. After each staining, the gels were visualized using the ChemiDoc MP imager.

Sample preparation for liquid chromatography mass spectrometry (LC-MS)

In vitro phosphorylation reactions of α_{s1}-casein with PrkD, PrkC, or YabT were performed as described above, using only non-radioactive ATP (10 mM). The resulting samples were digested on 30-kDa cut-off filter units (Millipore, MRCF0R030). In brief, samples were concentrated onto filters, washed twice with 200 µl of 8 M urea; 100 mM Tris-HCl pH 8.0 (UA buffer) and treated with 100 mM of DTT in UA for 30 min. Following another UA wash, samples were alkylated with 50 mM chloroacetamide in UA for 20 min in the dark. The samples were then equilibrated twice with 200 µl of 50 mM Tris pH 8.0 (digestion buffer) prior to protein digestion with Trypsin/LysC (Promega, 1:30 enzyme-to-protein ratio) for 16 hours at 37°C. Resulting peptides were C18 desalted prior to LC-MS/MS analysis.

LC-MS analysis of *in vitro* phosphorylated proteins

Peptides were loaded onto a 2 cm C18 trap column (ThermoFisher 164946), connected in-line to a 15 cm C18 reverse-phase analytical column (Thermo EasySpray ES904) using 100% Buffer A (0.1% Formic acid in water) at 750bar, using the Thermo EasyLC 1200 HPLC system, and the column oven operating at 30°C. Peptides were eluted over a 70 minute gradient ranging from 10% to 60% of Buffer B (80% acetonitrile, 0.1% formic acid) at 250 nl/min, and the Orbitrap Exploris instrument (Thermo Fisher Scientific) was run in DIA mode with FAIMS ProTM Interface (ThermoFisher Scientific) with CV of -45 V. Full MS spectra were collected at a resolution of 120,000, with an AGC target of 300% or maximum injection time set to 'auto' and a scan range of 400–1000 m/z. The MS2 spectra were obtained in DIA mode in the orbitrap operating at a resolution of 60.000, with an AGC target 1000% or maximum injection time set to 'auto', a normalized HCD collision energy of 32. The isolation window was set to 6 m/z with a 1 m/z overlap and window placement on. Each DIA experiment covered a range of 200 m/z resulting in three DIA experiments (400-600 m/z, 600-800 m/z and 800-1000 m/z). Between the DIA experiments a full MS scan is performed. MS performance was verified for consistency by running complex cell lysate quality control standards, and chromatography was monitored to check for reproducibility.

Analysis of proteomics data

The raw files were analyzed using SpectronautTM (version 17.1) and spectra were matched against the bovine α_{S1}-casein (P02662) protein sequence as well as the *E. coli* K-12 MG1655 (UP000000625) protein database (as background *E. coli* proteins stemming from Casein/kinase protein production were present in the samples). The data was searched with the BGS Phospho PTM workflow

with the following modifications. Acetyl (K) was added as a dynamic modification together with Oxidation (M), Phospho (STY) and Acetyl on protein N-termini. Cysteine carbamidomethyl was set as a static modification. The proteotypicity filter was set to only proteotypic and MS quantity level to MS1 and normalization deselected. The PTM probability cutoff was set to 0. Only phosphosites identified with a localization probability of >0.75 for at least one of the samples were considered localized.

In vitro digestion of recombinant α_{s1}-casein

The INFOGEST static *in vitro* digestion protocol [58] was adapted to assess the digestibility of recombinant α_{s1}-caseins. Commercially prepared simulated salivary fluid (SSF), simulated gastric fluid (SGF), and simulated intestinal fluid (SIF) from Biochemazone were used for the oral, gastric, and intestinal phases, respectively. 5 mL of protein samples (13.5 mg/mL) were first mixed with 5 mL of SSF (without α-amylase) and incubated at 37°C for 2 minutes with continuous shaking.

The gastric phase was initiated by adding 10 mL of SGF (pH 3.0) with pepsin (1 U/mL), followed by incubation at 37°C for 30 minutes. For the intestinal phase, 20 mL of SIF containing trypsin (0.05 U/mL), and bile salts (10 mM) was added, and the pH was adjusted to 7.0 using 1M NaOH. Samples were then incubated at 37°C for 30 minutes.

Aliquots were collected at 0, 1, 3, 5, 15, and 30 minutes during each phase, and digestion was terminated by heating samples at 95°C for 10 minutes. Protein degradation kinetics were analyzed using SDS-PAGE, with enzyme concentrations modified to enhance visualization of degradation patterns. The incubation duration was limited to 30 minutes due to rapid digestion of the proteins.

Calcium binding assay

The calcium-binding capacity assay was conducted following a previously published procedure with minor modifications [80]. Briefly, 1.0 mg/ml of phosphorylated α_{s1}-casein samples were dephosphorylated using FastAP (Thermo Scientific). The samples were prepared by mixing at a final concentration of 1 mg/ml with 1.145 mM $CaCl_2$ in FastAP buffer (100 mM Tris-HCl (pH 8.0), 50 mM $MgCl_2$, 1 M KCl, 0.2% Triton X-100 and 1mg/ml BSA). The solutions were agitated at 37°C for 2 hours, with the pH maintained at 8.0. The reaction mixtures were then filtered using Amicon Ultra centrifugal filters (Sigma-Aldrich) at 10,000 g at room temperature for 30 minutes. A $CaCl_2$ mixture without protein was used as a negative control for calculating the bound calcium. Calcium content was measured using the Calcium Colorimetric Assay Kit (MAK022, Sigma-Aldrich) at 575 nm, where the calcium ion concentration is determined by the chromogenic complex formed between free calcium ions and o-cresolphthalein.

Fluorescence spectroscopy

2D and 3D spectra of the recombinant proteins were carried out using FP-8550 spectrofluorometer (JASCO corporation, Tokyo, Japan) in right angle configuration. High precision quartz cell (art no. 104F-10-40) with a sample volume of 1 ml was used for the measurements. The samples were diluted to an A_{280} value of 0.08 for analysis. For recording the 3D spectra, the excitation range was 210-495 nm, and the emission range 230-520 nm with a step of 2 nm at 700 V and a scan speed 10000 nm/minute. For 2D spectra, the samples were excited at a wavelength of 275 and 290 nm with a step of 1 nm at 700 V and a scan speed of 500 nm/minute. The emission spectra of the buffer (50 mM MOPS) were measured to subtract its contribution from the sample's emission spectra. The fluorescence intensities of the tryptophan for each sample were normalized by dividing by the maximum intensity value of the dataset, enabling standardized comparisons across various conditions.

Particle size and electrophoretic mobility measurements

Particle size measurements by dynamic light scattering (DLS) was measured using Zetasizer Nano-Zs (Malvern Panalytical Ltd., Malvern, UK). A Greiner Bio-One semi-microcuvette was used with a sample concentration of 0.5 g/L and a volume of 600 µL. The temperature was varied from 10 to 50 °C with an interval of 5 °C. Three measurements were carried out with each for 10 runs, at a backscattering angle of 173°, and a position of 3 mm. The samples were equilibrated for 300 seconds between each measurement. The size peak volume of the proteins was analyzed.

QUANTIFICATION AND STATISTICAL ANALYSIS

The calcium binding assay was conducted with a sample size of three ($n = 3$). Measurements were taken from distinct samples, and statistical analysis was performed using a two-way ANOVA followed by Šídák's multiple comparisons test, based on means and standard deviations to test significance within and across the different groups. No data points were excluded from the analysis.